Japanese Journal of Radiology (2021) 39:984–993
https://doi.org/10.1007/s11604-021-01132-6

ORIGINAL ARTICLE

# Relationship between F-18 florbetapir uptake in occipital lobe and neurocognitive performance in Alzheimer's disease

**Tanyaluck Thientunyakit[1,6] · Thonnapong Thongpraparn[1] · Chakmeedaj Sethanandha[1] · Takahiro Yamada[2] · Yuichi Kimura[3] · Weerasak Muangpaisan[4] · Kazunari Ishii[2,5]**

Received: 10 February 2021 / Accepted: 5 May 2021 / Published online: 21 May 2021


## Abstract

**Purpose** To determine the association between occipital amyloid-PET uptake and neurocognitive performance in Alzheimer's disease (AD).

**Materials and methods** Fifty-eight participants with normal aged, mild cognitive impairment (MCI) due to AD and AD subjects who underwent F-18 florbetapir brain PET/CT scans were divided into four groups (A, normal; B, MCI; C, mild AD; and D, moderate/severe AD). Semiquantitative analyses of SUVR images were performed. The differences between groups and the correlations between florbetapir uptake and Thai Mental State Examination (TMSE) scores were determined. Significant differences were defined using a $P < 0.001$, uncorrected, or a $P < 0.05$, FWE for the voxel-based analyses with Statistical Parametric Mapping (SPM).

**Results** There was a slightly higher florbetapir uptake in the precuneus, parietal, and occipital association cortices in Group B > A. The occipital florbetapir uptake in Groups C and D was significantly higher than in Group A, in addition to the precuneus, anterior cingulate, posterior cingulate, temporoparietal, and frontal cortices. There was a strong negative correlation between TMSE scores and florbetapir uptake in the occipital lobe.

**Conclusions** Occipital amyloid uptake is associated with clinically advanced AD, and is inversely correlated with neurocognitive performance and may be useful for evaluating AD severity.

**Keywords** Alzheimer's disease · Amyloid PET · Florbetapir · Occipital

✉ Tanyaluck Thientunyakit
stanyalu@hotmail.com

1 Department of Radiology, Faculty of Medicine Siriraj Hospital, Mahidol University, 2 Wanglang, Siriraj, Bangkok Noi, Bangkok 10700, Thailand

2 Institute of Advanced Clinical Medicine, Kindai University Hospital, 377–2 Ohnohigashi, Osaka-Sayama, Osaka 589-8511, Japan

3 Graduate School of Biology-Oriented Science and Technology, Kindai University, 930 Nishimitani, Kinokawa City, Wakayama 649–6493, Japan

4 Department of Preventive and Social Medicine, Faculty of Medicine Siriraj Hospital, Mahidol University, 2 Wanglang, Siriraj, Bangkok Noi, Bangkok 10700, Thailand

5 Department of Radiology, Faculty of Medicine, Kindai University, 377–2 Ohnohigashi, Osaka-Sayama, , Osaka 589-8511, Japan

6 Division of Nuclear Medicine, Department of Radiology, Faculty of Medicine, Siriraj Hospital, 2 Wanglang Road, Bangkok Noi, Bangkok 10700, Thailand

## Introduction

Alzheimer's disease (AD) is the most common cause of dementia, which is estimated to affect approximately 5.8 million elderly people in the U.S. and 30 million people worldwide, with an increasing trend [1, 2]. It has been accepted that beta amyloid plaque aggregation is one of pathological hallmarks necessary for the diagnosis of AD. PET imaging biomarkers provide the potential for noninvasive, in vivo identification of beta amyloid pathology [3–5]. The uptake patterns in the neocortex observed by either C-11 or F-18 labeled amyloid-PET tracers have been proven to correspond well with the neuropathological distribution of amyloid beta plaque found in autopsies [4–6]. Moreover, the role of amyloid-PET imaging in AD diagnosis and management has recently been established [7–13].

F-18 florbetapir is an amyloid-PET tracer that rapidly enters the brain and specifically binds to cortical amyloid beta plaque [14]. There is evidence of a strong association

between the amyloid beta deposition estimated from florbetapir PET imaging (either visually or semiquantitatively, using the cortical-to-cerebellar standard uptake value ratio) and neuritic plaque density at autopsy, with high sensitivity, specificity, and accuracy [4]. However, the published data on florbetapir PET mostly focus on predefined, anatomically relevant cortical regions, namely, the frontal, temporal, parietal, anterior cingulate and posterior cingulate cortices and precuneus. These are the regions in which amyloid beta deposition is commonly found in patients with AD [4, 14–16]. Through our clinical work, we have observed that there is also a significant uptake of florbetapir at the occipital cortex. The presence of florbetapir occipital uptake in addition to the other associative neocortex, primary sensory–motor areas, and medial temporal lobe was previously classified as the most severe stage (stage IV) of in vivo amyloid burden [17]. Individuals with AD have a significantly higher amyloid burden than the mildly cognitively impaired or cognitively normal elderly. Furthermore, data from postmortem neuropathological studies support the view that AD-related changes are also involved in the occipital cortex [15, 18]. We hypothesize that beta amyloid deposition at the occipital cortex detected by florbetapir PET imaging might indicate a regional progression of advanced stage AD and correlate with the severity of neurocognitive impairment.

This study set out to compare beta amyloid deposition in the occipital cortex detected by florbetapir PET across a spectrum of elderly participants, ranging from those with normal cognition, to mild cognitive impairment (MCI) due to AD, to AD dementia with varying degrees of severity. We also explored the association between the occipital cortical amyloid-PET uptake and the level of neurocognitive performance.

## Materials and methods

This study was conducted with the prior approval of the Institutional Review Board (COA no. Si137/2015). All procedures performed in studies involving human participants were in accordance with the ethical standards of the institutional and/or national research committee and with the 1964 Helsinki declaration and its later amendments or comparable ethical standards.

### Participants

A total of 58 participants aged 60 and above who visited the geriatric clinic in single university hospital were enrolled. They were informed about the research protocols, and written consent to participate in the study was formally given by either the participants or their legally authorized representatives. FDG-PET/CT and florbetapir PET/CT scans of the brain were performed on all subjects between September 2016 and June 2018, and they were completed within 6 weeks of their neuropsychological assessments. Individuals were excluded from the study if they had an unstable medical condition; were seropositive for HIV or AIDS; abused drugs; had alcoholism, primary or metastatic brain cancer, significant brain lesions, or a history of amyloid-targeted medication usage; or were unwilling to follow the study protocol. The participants were divided into four groups, according to their clinical diagnoses and amyloid-PET results from visual interpretation. The clinical diagnoses were made by an experienced geriatrician (W.M.) using a combination of history, physical examination, and neurocognitive test results. The tests comprised the Thai Mental State Examination (TMSE) and clinical dementia rating (CDR) [16, 19, 20]. The TMSE was used to measure the cognitive function of the participants. It was developed in 1993 and was used in Thailand ever since [21]. The total score is 30 and the cut-off value for cognitive impairment is 23 or less. It includes assessment in orientation, memory (3-word registration and delayed recall), attention (days backward), calculation (100–7 subtraction), language ability (naming, sentence repetition, reading, 3-order command), picture copying, and abstract thinking (similarity). Previous studies in Thailand showed the distribution of norms of TMSE score in large Thai population (4459 people) which were varied depending on age and educational level [22]. The range of scores for normal cognition and AD was previously explored [23]. It was shown to have the excellent correlation (Pearson correlation 0.904) with the MMSE-Thai 2002, which is a Thai translated version of MMSE [24]. The severity of AD dementia was given a rating based on the TMSE score in accordance with an earlier publication [25] in combination with CDR. For this study, we focused on the subjects with AD pathology; therefore, positive amyloid-PET was included in the criteria for MCI and AD dementia groups to confirm AD continuum by biomarker as recently proposed by the National Institute on Aging and Alzheimer's Association (NIA-AA) [7]. The first of these group, "Group A", comprised 20 cognitively healthy controls (HC) (TMSE 24–30, CDR = 0) with negative amyloid-PET results. "Group B" was made up of 12 patients with MCI due to AD (TMSE 24–30, CDR 0.5) with positive amyloid-PET. "Group C" had 13 patients with mild AD dementia (TMSE > 20, CDR 0.5–1) showing positive amyloid-PET results. Finally, "Group D" consisted of 13 patients with moderate (TMSE 11–20, CDR 2)-to-severe AD dementia (TMSE ≤ 10, CDR 3) showing a positive amyloid-PET finding.

### PET imaging study

The synthesis of florbetapir PET tracer and florbetapir PET imaging protocol were described in our previous work [19]. Briefly, a 20-min dynamic amyloid-PET/CT brain image

was acquired 50 min after an intravenous injection of 10 mCi (370 MBq) florbetapir, using a Discovery STE PET/CT scanner (GE Healthcare, WI, USA). An F-18 FDG-PET/CT scan of the brain was also performed using the same scanner, with a 30-min dynamic acquisition 30 min after the intravenous injection of 4.5–5.5 mCi (166.5 –203.5 MBq) FDG. The detailed image acquisition and reconstruction protocols were as stated in our previous work and in Alzheimer's Disease Neuroimaging Initiative 2 [19, 26]. The interval for both PET/CT scans was at least 24 h.

## PET image analysis

The visual interpretation of amyloid-PET in all cases was previously performed in consensus by 2 board-certified, nuclear medicine physicians (T.T. and C.S.) trained in amyloid-PET interpretation using the original PET images without the knowledge of clinical information and the interpretation data were recorded. Using previously recommended criteria [4, 9], the amyloid-PET images of each participant were classified as either "amyloid positive" or "amyloid negative". The amyloid-positive images showed increased amyloid retention in the cortical gray matter, with a loss of gray–white matter contrast in at least 2 cortical regions, or an intense uptake in at least 1 cortical region. By contrast, the amyloid-negative images demonstrated no, or low, amyloid retention in the cortical gray matter.

A further semi-quantitative analysis was performed on all PET studies using Statistical Parametric Mapping (SPM) version 12 (The Wellcome Centre for Human Neuroimaging, UCL Queen Square Institute of Neurology, London, UK, available at https://www.fil.ion.ucl.ac.uk/spm/software/spm12/) [27], as follows. Initially, all cases of florbetapir and FDG-PET images were converted from DICOM to Nifti format by dcm2niiGUI application (NeuroImaging Tools & Resources Collaboratory). Florbetapir-FDG coregistered images were created and normalized by TPM (tissue probability maps) template in the next step [28, 29]. In addition, the normalized SUV images were smoothed, and the mean florbetapir cortical-to-cerebellar standard uptake value ratio (SUVR) images were performed by dividing them with the cerebellar ROI template, which was drawn on the cerebellar area (the cerebellum was the reference region) [30]. The SUVR images, which were created from original images in all cases, were evaluated again by senior nuclear medicine physician (K.I.) to confirm the results from visually read amyloid-PET. The ROI for reference area (cerebellum) was originally drawn by 1 senior nuclear medicine physician (K.I.) in the TPM.nii template for using with SPM (Fig. 1). Using this cerebellar ROI template, the cerebellar counts were calculated at each individual anatomically standardized image automatically, and then using this value, each individual SUVR image was created by 1 physicist (T.T.). The semi-quantitative analysis was performed by 2 independent operators (T.T. and K.I.) with same analytical results to ensure the reproducibility of the results. For the voxel-based analysis by SPM, one-way Analysis of Variance (ANOVA) tests were performed among the four groups, and correlation analyses between the regional florbetapir uptake and TMSE scores were performed. FDG-PET images were also analyzed in the same way.

## Statistical analysis

The differences between the baseline characteristics and the amyloid depositions of the groups were evaluated using Pearson's Chi-squared and one-way ANOVA, with a post hoc analysis using the Bonferroni test. Pearson's correlation between the cortical amyloid and FDG uptakes and the levels of neurocognitive performance using the TMSE scores was also assessed. A significant difference was defined using a $P$ value of $< 0.05$. For SPM statistics, the threshold for significant difference was set as $P < 0.001$, uncorrected, for the one-way ANOVA of the 4-group comparisons, and $P < 0.05$, Family-Wise Error (FWE), for the correlation analysis.

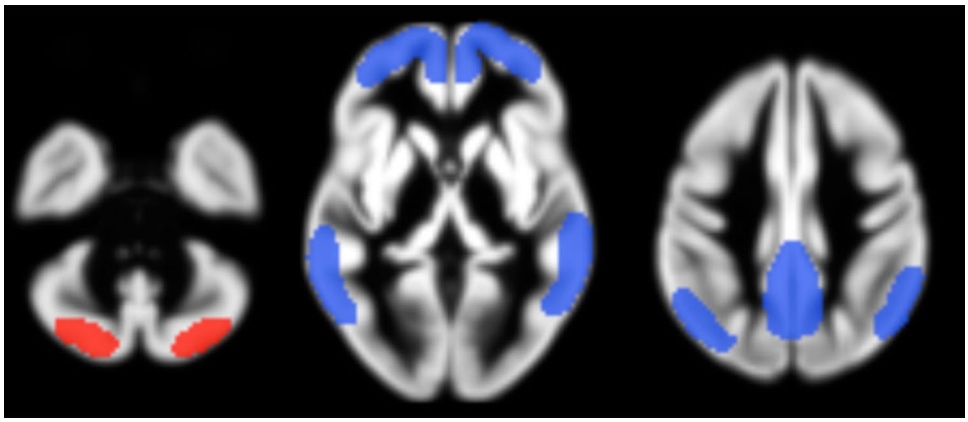

**Fig. 1** The ROIs over the bilateral cerebellum (in red) and bilateral cerebral cortices (in blue) for further analysis of regional cerebellar-normalized SUVR

## Results

The baseline characteristics of all participant groups are listed in Table 1. There were no significant differences in the age, gender, or years of education of the subjects in the four groups. As predicted, significant differences between the TMSE and CDR scores were found between Groups A versus D, A versus B, and C versus D. Significant differences in the E4 variant of Apolipoprotein E (APOE4) carriers of the groups were also found, with Group C having the highest percentage.

The differences in the cortical amyloid depositions and FDG uptake of the patient groups (Groups B to D) relative to the normal control (Group A) are pictorialized in Fig. 2. There was a slightly higher cortical uptake of florbetapir in the visual association (BA19) and parietal cortices, anterior prefrontal /anterior cingulate cortices (BA10), the precuneus (BA7), and temporal cortices (BA21) in Group B than in Group A (Fig. 2a). However, compared with Group A, the cortical amyloid deposition in Group C was significantly higher in the occipital cortex (BA19, BA17) as well as being significantly higher in the precuneus (BA7), anterior cingulate (BA32), posterior cingulate (BA23, BA31), temporoparietal (BA22, BA39), and frontal cortices (BA11) (Fig. 2b). A similar pattern was also detected when Group D was compared with Group A, but with slightly more extensive regions and with higher amyloid depositions, including in the lateral and medial occipital cortices (BA 17 and 18) (Fig. 2c). Details of the locations of the regions showing significantly increased florbetapir uptake in the Group A-to-D subjects are given in Table 2. The regions located in occipital lobe (BA17, BA18, and BA19) partly show higher amyloid deposition in every group comparison. The box-and-whisker plot graph of mean and SD of each group's mean cortical SUVR is also demonstrated (Fig. 2d).

Concerning glucose metabolism: FDG uptake, in Group B, only posterior cingulate metabolism was decreased (Fig. 3a), while the bilateral parietal, frontal, and posterior cingulate metabolism were decreased in Group C (Fig. 3b) and the bilateral parietotemporal, frontal, and posterior cingulate metabolism were decreased in Group D (Fig. 3c).

When we first estimated the amyloid deposit correlation using threshold $P < 0.001$, uncorrected almost the whole brain area was negatively correlated, but the occipital cortices had the strongest correlation (Fig. 4). Then, after using strict criteria $P < 0.05$, FWE, only the occipital cortices survived (Fig. 5; Table 3). Significant correlations between FDG uptake and TMSE were demonstrated in the bilateral parietotemporal and frontal as sociation, posterior cingulate, and precuneus cortices (Fig. 6).

## Discussion

The areas known for potentially intense amyloid loads, as evident by brain autopsies of patients with AD, are the middle frontal gyrus, anterior cingulate cortex, and posterior cingulate cortex. Much lower amyloid loads are found in the occipital cortex, hippocampus, and parahippocampal gyri; the remaining areas of the brain are amyloid negative. The mean florbetapir SUVRs of the frontal, temporal, parietal, anterior cingulate, and posterior cingulate cortices, and the precuneus were higher in AD patients than in the normal control [14], but not in the occipital cortices. The cerebellar-normalized occipital SUVR of the AD group was slightly higher than those of the MCI and control groups [31], which correspond with our results. A higher mean cerebellar-normalized SUVR for the occipital cortex in the amyloid-PET positive AD and MCI groups than in the amyloid-PET negative MCI and HC groups was reported [32]. Moreover, the occipital cortex was the fourth region with highest discrimination ability to differentiate AD from

**Table 1** Comparison of characteristics of participants in all three groups

| Characteristics | A ($n=20$) | B ($n=12$) | C ($n=13$) | D ($n=13$) | *P* value |
|---|---|---|---|---|---|
| Age (years), mean ± SD | 69.20 ± 5.28 | 69.17 ± 3.81 | 70.85 ± 7.68 | 70.85 ± 5.37 | 0.748 |
| Gender (% female) | 65.0% | 41.6% | 58.3% | 58.3% | 0.640 |
| Education (years), mean ± SD | 12.50 ± 5.92 | 14.25 ± 3.77 | 14.69 ± 3.30 | 9.62 ± 5.99 | 0.057 |
| Onset of symptoms (months), mean ± SD | – | 17.33 ± 9.64 | 32.77 ± 20.11 | 42.54 ± 17.59 | 0.000[a,b,c] |
| TMSE, mean ± SD | 27.95 ± 1.67 | 26.83 ± 1.90 | 25.62 ± 1.45 | 18.15 ± 4.26 | 0.000[c] |
| CDR, mean ± SD | 0.00 ± 0.00 | 0.5 ± 0.00 | 0.54 ± 0.14 | 1.16 ± 0.42 | 0.000[a,b,c] |
| APOE4 carrier (%) | 11.8% | 41.7% | 75.0% | 30% | 0.006 |

*A* HCs with negative amyloid-PET, *B* MCIs suspected due to AD with positive amyloid-PET, *C* very mild AD and positive amyloid-PET, *D* mild-to-severe AD and positive amyloid-PET, *TMSE* Thai Mental State Examination, *CDR* clinical dementia rating

Post hoc test results: [a]significant difference found between Groups A and B; [b]significant difference found between Groups A and C; [c]significant difference found between Groups A and D

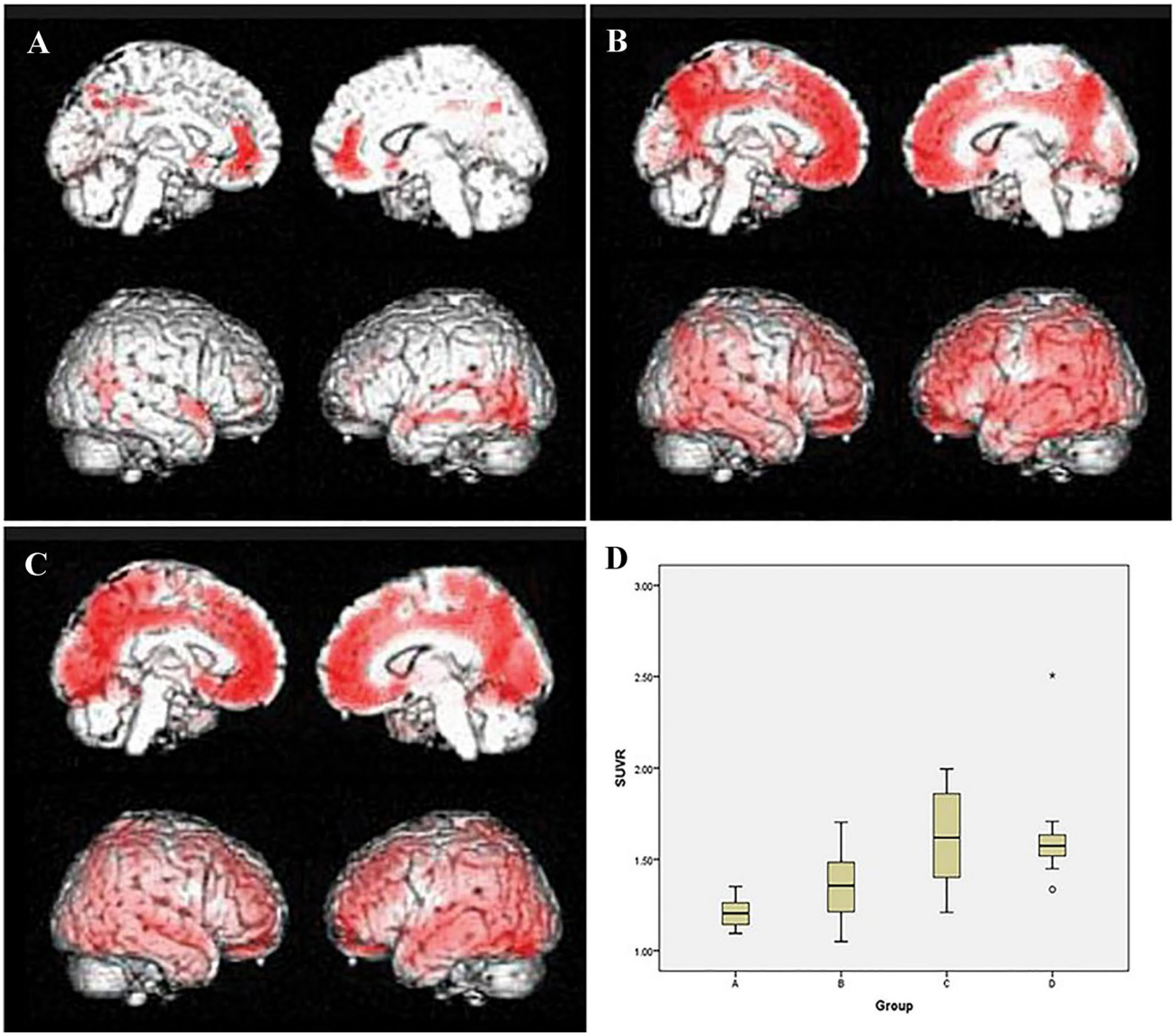


**Fig. 2** Comparison of the regional amyloid deposition across participants in Groups A–D. There was no significant difference in occipital amyloid deposition between Groups A and B (**a**). However, significantly higher cortical amyloid deposition at the occipital cortex was noted in both Groups C (**b**) and D (**c**), relative to Group A, in addition to other regions, namely, the precuneus, anterior cingulate, posterior cingulate, temporoparietal, and frontal cortices ($P < 0.001$, uncorrected). The box-and-whisker plot graph shows mean and SD of each group's mean cortical SUVR (2D)

HC. The higher stage of amyloid loads (stage IV), which was characterized by amyloid deposition in the occipital lobe and striatum in addition to the areas of the brain involved in earlier stages, showed association with the worsened cognition [17]. Unfortunately, other florbetapir studies [4, 30, 33–35] did not include the occipital regions in their evaluations. Apart from florbetapir, higher C-11 PIB SUVRs were demonstrated in the occipital cortices in the amyloid-PET positive A D and MCI groups than in the amyloid-PET negative MCI and HC groups as well as its high discrimination ability to differentiate between AD and HC [32]. A significantly higher C-11 PIB accumulation in the occipital cortices of AD subjects was also demonstrated [36]. Higher occipital florbetaben PET uptakes were also observed in the AD group than in the normal control group [5, 37, 38]. The currently available published data on F-18 flutemetamol do not include any specific information on the occipital uptake of participants with different neurocognitive performance levels [39–41].

The current role of beta amyloid-PET study is early detection and prediction of disease progression. The possible explanations for discordance between regional amyloid

**Table 2** Representative location of regions showing extremely increased florbetapir uptake among the A-to-D group subjects (Note to publisher: I would like to have each numeric content in the 2nd (or 3rd) to 6th columns to be positioned in the center of cell, if possible)

| Brain region | Side | Coordinates | | | *T* values |
|---|---|---|---|---|---|
| | | *X* | *Y* | *Z* | |
| B > A group | | | | | |
| Visual association cortex (BA19) | Lt | −40 | −73 | 1 | 5.01 |
| Visual association cortex (BA19) | Rt | 46 | −59 | 11 | 4.90 |
| Anterior prefrontal cortex (BA10)/anterior cingulate cortex (BA32) | Rt | 5 | 41 | −4 | 4.43 |
| Middle temporal gyrus (BA21) | Lt | −60 | −24 | −12 | 4.11 |
| Precuneus (BA7) | Lt | −8 | −64 | 43 | 3.95 |
| C > A group | | | | | |
| Angular gyrus (BA39) | Rt | 33 | −66 | 42 | 7.54 |
| Superior temporal gyrus (BA22) | Lt | −56 | −41 | 19 | 7.24 |
| Visual association cortex (BA19) | Lt | −41 | −71 | 3 | 7.14 |
| Orbitofrontal area (BA11) | Lt | −2 | 35 | −12 | 6.06 |
| Posterior cingulate cortex (BA23) | Lt | −1 | −44 | 32 | 5.94 |
| Primary visual cortex (BA17) | Rt | 8 | −88 | 0 | 4.07 |
| D > A group | | | | | |
| Orbitofrontal area (BA11) | Rt | 0 | 33 | −9 | 7.86 |
| Orbitofrontal area (BA11) | Rt | 3 | 39 | −4 | 7.81 |
| Fusiform gyrus | Lt | −43 | −64 | 0 | 7.71 |
| Visual association cortex (BA19) | Lt | −44 | −72 | 0 | 6.92 |
| Posterior cingulate cortex (BA31) | Lt | −5 | −45 | 39 | 5.84 |
| Angular gyrus (BA39) | Rt | 34 | −72 | 47 | 4.14 |
| Primary visual cortex (BA17) | Rt | 8 | −85 | 0 | 3.75 |

Threshold is $p < 0.001$, uncorrected

*Lt.* Left, *Rt.* right

deposition, tau deposition, and glucose hypometabolism revealed from PET studies include role of time, remote effect, and different threshold of imaging modalities [19]. Although there were some data supporting the relationship between amyloid deposition and the severity of AD dementia [17, 19, 42, 43], they seem relatively limited when compared to the same relationship with the abnormality detected by Tau PET or FDG-PET. This lack of correlation may be partly explained by the criteria for interpretation of amyloid-PET as binary scale. Moreover, the occipital lobe is not included in the representative areas of the beta amyloid deposition known to be associated with cognitive function, although it is not uncommon to detect a higher amyloid load in the occipital region in AD than in MCI and/or normal controls [31, 32, 36–38]. The higher occipital amyloid deposition in MCI and AD cohorts and its tendency to associated with lower neurocognitive scores in our initial works [19, 44] motivated us to explore the potential role of beta amyloid-PET study as the marker for disease severity in AD, as well as predictor for progression of cognitive impairment specifically in amyloid-positive subjects. To our knowledge, there has been no report on the relationship between the occipital amyloid load and the level of neurocognitive performance. We found a strongly negative correlation between the florbetapir occipital cortical uptake and the level of neurocognitive performance, determined using TMSE scores. This relationship might be explained by the tendency to have a higher occipital cortex involvement in the later stages of AD, based on the evidence from neuropathological assessments [15], which is possibly related to the long-standing of AD pathology occurs in the brain resulted in increased severity of AD (or so-called advance stage of AD), which more cortical areas including frontal and occipital cortices also get amyloid deposits. As a result, high occipital amyloid plaque deposition—as evidenced by PET biomarkers—is probably associated with the more advanced stages of AD. Another possible explanation for this observation is that florbetapir has a greater tendency than either C-11 PiB or F-18 flutemetamol to accumulate in the occipital lobe. For a visual interpretation of florbetapir and florbetaben, evaluation of the gray matter uptake is performed in the temporal, parietal, frontal, and occipital regions. On the other hand, in flutemetamol, the striatum is evaluated in addition to the temporal, frontal, and parietal regions, while the occipital region is not included [45]. It is known that flutemetamol accumulates in the striatum following the amyloid deposition stage but not predominant in the occipital lobe [46], unlike our results, which florbetapir accumulates in the occipital lobe following the amyloid deposition stage but not predominant in the striatum. There has been no study to directly compare the differences in distribution between these two radiotracers in the same individuals. However, the distribution of each radiotracer uptake to reflect the beta amyloid deposition were obtained from previous publications, and generally in accordance with the affected areas confirmed by pathological assessment. The different chemical structures among the F-18 amyloid tracers likely affecting affinities to deposited beta amyloid in the brain and resulting in different uptake patterns. We hypothesize that florbetapir has a binding affinity in the occipital lobe, which can be detected at a relatively advanced stage of amyloid deposition and probably used as a similar marker to an increased tau PET uptake or an inversed FDG-PET uptake, the markers of which are known to correlate better with the degree

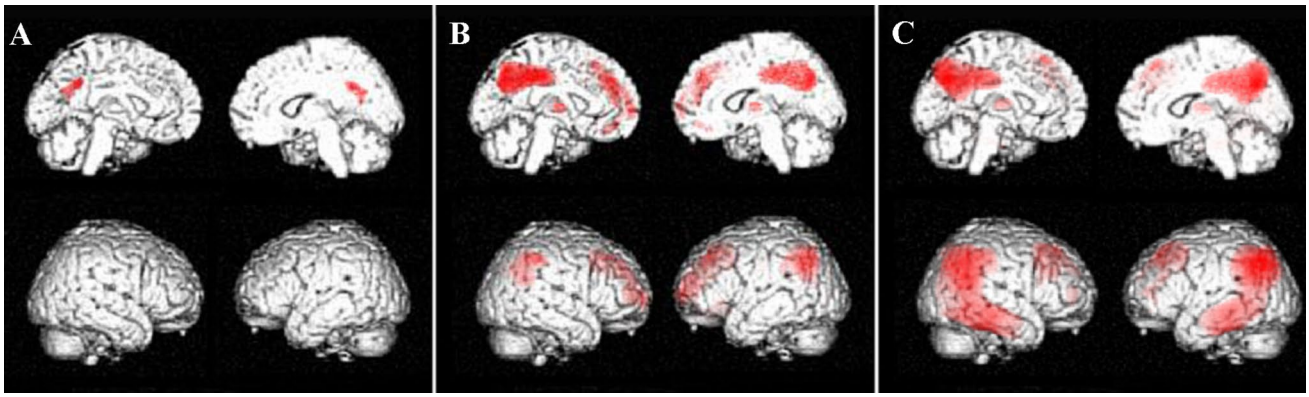


**Fig. 3** Comparison of the regional glucose metabolism across participants in Groups A–D. There was a significant metabolic decrease in posterior cingulate cortices between Groups A and B (**a**). Posterior cingulate, precuneus, parietal association, and frontal association cortical metabolism were significantly decreased in both Groups C (**b**) and D (**c**); in addition to the regions, temporal association cortical metabolism was significantly decreased in Group D (**c**) ($P < 0.001$, uncorrected)

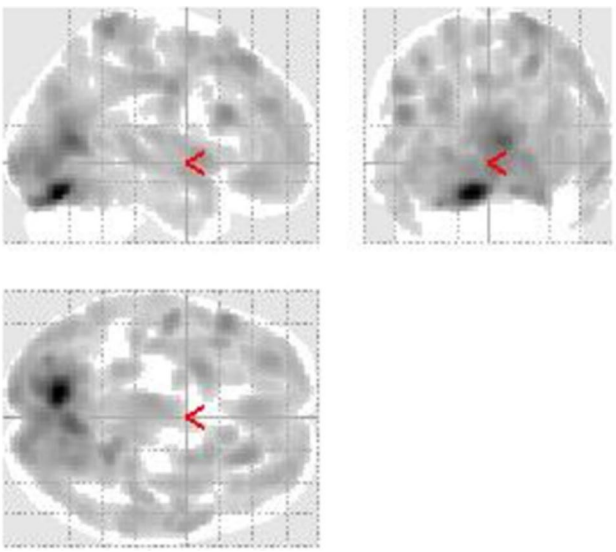

**Fig. 4** The voxel-based analysis from florbetapir PET data in all 58 participants resulted in negative correlation between cerebral cortical uptake and the TMSE score ($P < 0.001$, uncorrected). Note that almost the whole cerebral cortices were negatively correlated with TMSE score, but the occipital cortices had the strongest correlation

of cognitive impairment. In our study, posterior cingulate is the first abnormal region to be involved both in florbetapir and FDG-PET, and then, other regions namely, frontal, parietal, and precuneus are affected, though the degree of involvement is different.

One limitation of this study is its small sample size, which may affect its statistical power. Moreover, we used only the total TMSE score to assess the correlation between the occipital cortical uptake and neurocognitive performance. Therefore, a further investigation with a larger cohort as well as correlations with more detailed neurocognitive tests are needed to confirm the significance of the occipital amyloid-PET uptake. Also, we cannot verify via histopathological examination that the occipital florbetapir uptake really demonstrates amyloid beta accumulation. A consistent regional hierarchy of amyloid deposition has been demonstrated in a large series of florbetapir PET scans across the full clinical spectrum of AD, strongly indicating that PET-measured amyloid deposition follows a predictable regional sequence that can be used analogously to established neuropathologic approaches for staging an individual's pathologic state along this sequence. [17] Finally, there are other known potential causes for amyloid deposition in the occipital lobe, namely posterior cortical atrophy, DLB, and cerebral amyloid angiopathy. Nevertheless, we correlated results from MRI and FDG-PET in all subjects to confirm that there were no specific abnormalities that may indicate those diseases, either by structural dominant parieto-occipital lobe and visual association cortex atrophy or blooming artifacts due to microbleeds, or by the pattern of glucose metabolic abnormality. Although occipital amyloid uptake should be interpreted in combination with the other regions of amyloid deposition, its presence may indicate a higher dynamic range at the clinically overt AD stages. The findings may also prove more useful than the global cortical amyloid-PET uptake for stratifications of the severity of preclinical AD and predictions of the level of neurocognitive impairment.

## Conclusions

Amyloid plaque deposition in the occipital cortex, as evidenced via F-18 florbetapir PET, is associated with clinically advanced Alzheimer's dementia, and it inversely correlates with the level of neurocognitive performance. The presence

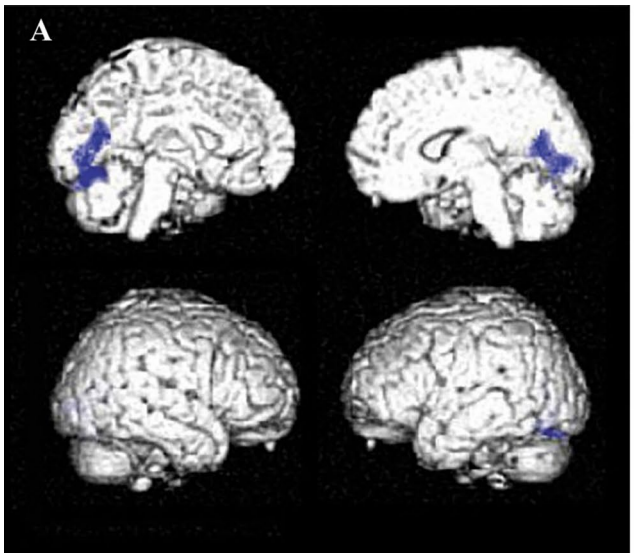


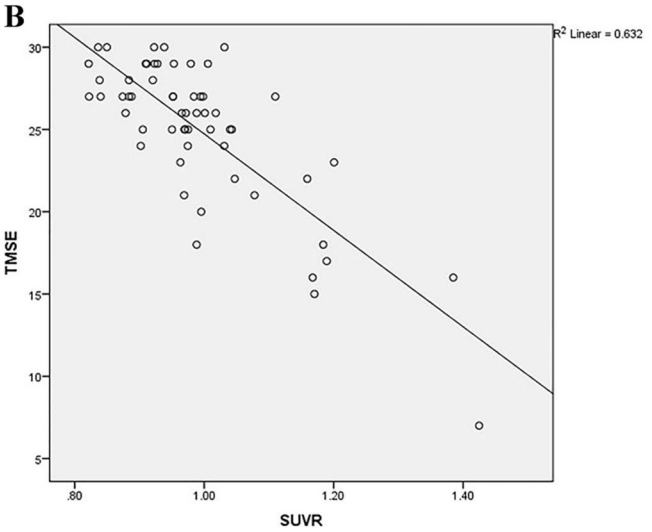


**Fig. 5** The voxel-based analysis from florbetapir PET data in all 58 participants resulted in a strong negative correlation between the occipital cortical uptake and the TMSE score ($P < 0.05$, FWE) (a). Scatter-plot graph shows the relationship between the occipital SUVR (*x*) and TMSE scores (*y*) in all subjects (**b**)

**Table 3** Statistically significant correlations between florbetapir uptake and TMSE (Note to publisher: I would like to have the content in the 2nd to 6th columns to be positioned in the center of cell, if possible)

| Brain region | Side | Coordinates | | | *T* values |
|---|---|---|---|---|---|
| | | *X* | *Y* | *Z* | |
| Visual association cortex (BA18) | Lt | −11 | −70 | −4 | 8.36 |
| Visual association cortex (BA18) | Rt | 6 | −64 | 10 | 6.53 |
| Primary visual cortex (BA17) | Lt | 16 | −87 | 2 | 5.51 |

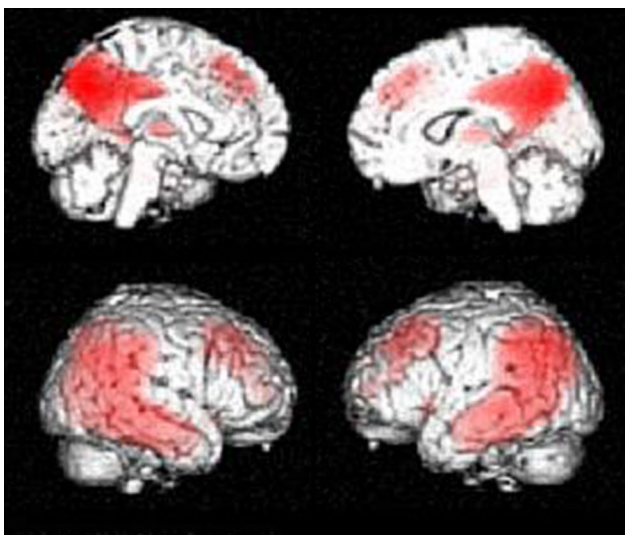

**Fig. 6** The voxel-based analysis demonstrated that posterior cingulate, precuneus, parietotemporal, and frontal association cortices glucose metabolism well correlates with TMSE score ($P < 0.05$, FWE)

of occipital amyloid-PET uptake may be useful for evaluating the severity of AD.

**Acknowledgements** The authors thank Phattaranan Phawaphutanon, Angkana Jongsawadipatana, and Dollaporn Polyeum for the data collection, and the staff at the Division of Nuclear Medicine, Department of Radiology and at the Department of Preventive and Social Medicine for their technical assistance. This work was partially funded by National Research Council of Thailand through Health System Research Institute (Grant Nos. 58–036, 60–065, and 62–044), Research Development Fund, Faculty of Medicine Siriraj Hospital (Grant Nos. R016236003 and R016134004), and the International Atomic Energy Agency under CRP E13043 (Grant No. 19256).

**Author contributions** Conceptualization: TT and KI. Methodology: TT, CS, WM, and KI. Formal analysis and investigation: TT, TT, CS, WM, and KI. Writing—original draft preparation: TT. Writing—review and editing: TT, CS, WM, TY, YK, and KI. Funding acquisition: TT and WM. Resources: TT, CS, and WM. Supervision; KI.

**Funding** This work was partially funded by National Research Council of Thailand through Health System Research Institute (Grant Nos. 58–036, 60–065, and 62–044), Research Development Fund, Faculty of Medicine Siriraj Hospital (Grant Nos. R016236003 and R016134004), and the International Atomic Energy Agency under CRP E13043 (Grant No. 19256).

## Declarations

**Conflict of interest** No conflicts of interest related to any aspect of this study.

## References


1. Alzheimer's Association. 2019 Alzheimer's disease facts and figures. Alzheimers Dement. 2019;15:321–87.
2. Holtzman DM, Morris JC, Goate AM. Alzheimer's disease: the challenge of the second century. Sci Transl Med. 2011;3:77.
3. Hyman BT, Phelps CH, Beach TG, Bigio EH, Cairns NJ, Carrillo MC, et al. National Institute on Aging–Alzheimer's Association guidelines for the neuropathologic assessment of Alzheimer's disease. Alzheimers Dement. 2012;8:1–13.
4. Clark CM, Pontecorvo MJ, Beach TG, Bedell BJ, Coleman RE, Doraiswamy PM, et al. Cerebral PET with florbetapir compared with neuropathology at autopsy for detection of neuritic amyloid-β plaques: a prospective cohort study. Lancet Neurol. 2012;11:669–78.
5. Sabri O, Sabbagh MN, Seibyl J, Barthel H, Akatsu H, Ouchi Y, et al. Florbetaben PET imaging to detect amyloid beta plaques in Alzheimer's disease: phase 3 study. Alzheimers Dement. 2015;11:964–74.
6. Curtis C, Gamez JE, Singh U, Sadowsky CH, Villena T, Sabbagh MN, et al. Phase 3 trial of flutemetamol labeled with radioactive fluorine 18 imaging and neuritic plaque density. JAMA Neurol. 2015;72:287–94.
7. Jack CR Jr, Bennett DA, Blennow K, Carrillo MC, Dunn B, Haeberlein SB, et al. NIA-AA research framework: toward a biological definition of Alzheimer's disease. Alzheimers Dement. 2018;14:535–62.
8. Frisoni GB, Boccardi M, Barkhof F, Blennow K, Cappa S, Chiotis K, et al. Strategic roadmap for an early diagnosis of Alzheimer's disease based on biomarkers. Lancet Neurol. 2017;16:661–76.
9. Johnson KA, Minoshima S, Bohnen NI, Donohoe KJ, Foster NL, Herscovitch P, et al. Appropriate use criteria for amyloid PET: a report of the Amyloid Imaging Task Force, the Society of Nuclear Medicine and Molecular Imaging, and the Alzheimer's Association. J Nucl Med. 2013;54:476–90.
10. Barthel H, Sabri O. Clinical use and utility of amyloid imaging. J Nucl Med. 2017;58:1711–7.
11. Shea Y-F, Barker W, Greig-Gusto MT, Loewenstein DA, Duara R, DeKosky ST. Impact of amyloid PET imaging in the memory clinic: a systematic review and meta-analysis. J Alzheimers Dis. 2018;64:323–35.
12. Rabinovici GD, Gatsonis C, Apgar C, Chaudhary K, Gareen I, Hanna L, et al. Association of amyloid positron emission tomography with subsequent change in clinical management among Medicare beneficiaries with mild cognitive impairment or dementia. JAMA. 2019;321:1286–94.
13. Villemagne VL, Klunk WE, Mathis CA, Rowe CC, Brooks DJ, Hyman BT, et al. Aβ Imaging: feasible, pertinent, and vital to progress in Alzheimer's disease. Eur J Nucl Med Mol Imaging. 2012;39:209–19.
14. Wong DF, Rosenberg PB, Zhou Y, Kumar A, Raymont V, Ravert HT, et al. In vivo imaging of amyloid deposition in Alzheimer disease using the radioligand 18F-AV-45 (flobetapir F 18). J Nucl Med. 2010;51:913–20.
15. Braak H, Braak E. Neuropathological stageing of Alzheimer-related changes. Acta Neuropathol. 1991;82:239–59.
16. Consensus recommendations for the postmortem diagnosis of Alzheimer's disease. The National Institute on Aging, and Reagan Institute Working Group on diagnostic criteria for the neuropathological assessment of Alzheimer's disease. Neurobiol Aging. 1997; 18:S1–S2
17. Grothe MJ, Barthel H, Sepulcre J, Dyrba M, Sabri O, Teipel SJ, et al. In vivo staging of regional amyloid deposition. Neurology. 2017;89:2031–8.
18. Thal DR, Rüb U, Orantes M, Braak H. Phases of Aβ-deposition in the human brain and its relevance for the development of AD. Neurology. 2002;58:1791–800.
19. Thientunyakit T, Sethanandha C, Muangpaisan W, Chawalparit O, Arunrungvichian K, Siriprapa T, et al. Relationships between amyloid levels, glucose metabolism, morphologic changes in the brain and clinical status of patients with Alzheimer's disease. Ann Nucl Med. 2020;34:337–48.
20. McKhann GM, Knopman DS, Chertkow H, Hyman BT, Jack CR Jr, Kawas CH, et al. The diagnosis of dementia due to Alzheimer's disease: recommendations from the National Institute on Aging-Alzheimer's Association workgroups on diagnostic guidelines for Alzheimer's disease. Alzheimers Dement. 2011;7:263–9.
21. Train the Brain Forum Committee. Thai mental state examination (TMSE). Siriraj Hosp Gaz. 1993;45:661–74.
22. Muangpaisan W, Assantachai P, Sitthichai K, Richardson K, Brayne C. The distribution of Thai Mental State Examination Scores among Non-Demented Elderly in Suburban Bangkok Metropolitan and Associated Factors. J Med Assoc Thai. 2015;98:916–24.
23. Phannarus H, Muangpaisan W, Siritipakorn P, Chotinaiwattarakul W. Cognitive profiles and optimal cut-offs for routine cognitive tests in elderly individuals with Parkinson's disease, Parkinson's disease dementia, Alzheimer's disease, and normal cognition. Psychogeriatrics. 2020;20:20–7.
24. Institute of Geriatric Medicine, Department of Medical Services, Ministry of Public Health. The association between MMSE-Thai 2002 and Thai Mini-Mental State Examination; TMSE in the screening for dementia in elderly. http://agingthai.dms.moph.go.th/agingthai/wp-content/uploads/2020/04/โครงการประเมินเทคโนโลยีทางการแพทย์.pdf (Thai). Accessed 10 Oct 2020
25. Perneczky R, Wagenpfeil S, Komossa K, Grimmer T, Diehl J, Kurz A. Mapping scores onto stages: mini-mental state examination and clinical dementia rating. Am J Geriat Psychiat. 2006;14:139–44.
26. Alzheimer's Disease Neuroimaging Initiative website. ADNI 2 PET technical procedures manual: Florbetapir. http://www.adni-info.org/Scientists/doc/ADNI2_PET_Tech_Manual-Version_4_2014Oct27_CLEAN.pdf
27. Penny WD, Friston KJ, Ashburner JT, Kiebel SJ, Nichols TE. Statistical parametric mapping: the analysis of functional brain images. London: Elsevier; 2007.
28. Prieto E, Collantes M, Delgado M, Juri C, García-García L, Molinet F, et al. Statistical parametric maps of 18 F-FDG PET and 3-D autoradiography in the rat brain: a cross-validation study. Eur J Nucl Med Mol Imaging. 2011;38:2228–37.
29. Jones G, Ellis KA, Ames D, Martins RN, Eustache F, Salvado O, et al. Regional dynamics of amyloid-b deposition in healthy elderly, mild cognitive impairment and Alzheimer's disease: a voxelwise PiB–PET longitudinal study. Brain. 2012;135:2126–39.
30. Joshi AD, Pontecorvo MJ, Clark CM, Carpenter AP, Jennings DL, Sadowsky CH, et al. Performance characteristics of amyloid PET with florbetapir F 18 in patients with Alzheimer's disease and cognitively normal subjects. J Nucl Med. 2012;53:378–84.
31. Camus V, Payoux P, Barré L, Desgranges B, Voisin T, Tauber C, et al. Using PET with 18 F-AV-45 (florbetapir) to quantify brain amyloid load in a clinical environment. Eur J Nucl Med Mol Imaging. 2012;39:621–31.
32. Chiotis K, Carter SF, Farid K, Savitcheva I, Nordberg A. Amyloid PET in European and North American cohorts; and exploring age as a limit to clinical use of amyloid imaging. Eur J Nucl Med Mol Imaging. 2015;42:1492–506.
33. Clark CM, Schneider JA, Bedell BJ, Beach TG, Bilker WB, Mintun MA, et al. Use of florbetapir-PET for imaging β-amyloid pathology. JAMA. 2011;305:275–83.

34. Johnson KA, Sperling RA, Gidicsin CM, Carmasin JS, Maye JE, Coleman RE, et al. Florbetapir (F18-AV-45) PET to assess amyloid burden in Alzheimer's disease dementia, mild cognitive impairment, and normal aging. Alzheimers Dement. 2013;9:S72–83.
35. Namiki C, Takita Y, Iwata A, Momose T, Senda M, Okubo Y, et al. Imaging characteristics and safety of florbetapir (18 F) in Japanese healthy volunteers, patients with mild cognitive impairment and patients with Alzheimer's disease. Ann Nucl Med. 2015;29:570–81.
36. Nordberg A, Carter SF, Rinne J, Drzezga A, Brooks DJ, Vandenberghe R, et al. A European multicentre PET study of fibrillar amyloid in Alzheimer's disease. Eur J Nucl Med Mol Imaging. 2013;40:104–14.
37. Rowe CC, Ackerman U, Browne W, Mulligan R, Pike KL, O'Keefe G, et al. Imaging of amyloid β in Alzheimer's disease with 18F-BAY94-9172, a novel PET tracer: proof of mechanism. Lancet Neurol. 2008;7:129–35.
38. Becker GA, Ichise M, Barthel H, Luthardt J, Patt M, Seese A, et al. PET quantification of 18F-florbetaben binding to β-amyloid deposits in human brains. J Nucl Med. 2013;54:723–31.
39. Nelissen N, Van Laere K, Thurfjell L, Owenius R, Vandenbulcke M, Koole M, et al. Phase 1 study of the Pittsburgh compound B derivative 18F-flutemetamol in healthy volunteers and patients with probable Alzheimer disease. J Nucl Med. 2009;50:1251–9.
40. Vandenberghe R, Van Laere K, Ivanoiu A, Salmon E, Bastin C, Triau E, et al. 18F-flutemetamol amyloid imaging in Alzheimer disease and mild cognitive impairment: a phase 2 trial. Ann Neurol. 2010;68:319–29.
41. Miki T, Shimada H, Kim J-S, Yamamoto Y, Sugino M, Kowa H, et al. Brain uptake and safety of Flutemetamol F 18 injection in Japanese subjects with probable Alzheimer's disease, subjects with amnestic mild cognitive impairment and healthy volunteers. Ann Nucl Med. 2017;31:260–72.
42. Cohen AD, Rabinovici GD, Mathis CA, Jagust WJ, Klunk WE, Ikonomovic MD. Using Pittsburgh Compound B for in vivo PET imaging of fibrillar amyloid-beta. Advances in pharmacology. Amsterdam: Elsevier; 2012. p. 27–81.
43. Pike KE, Savage G, Villemagne VL, Ng S, Moss SA, Maruff P, et al. β-amyloid imaging and memory in non-demented individuals: evidence for preclinical Alzheimer's disease. Brain. 2007;130(11):2837–44.
44. Thientunyakit T, Sethanandha C, Muangpaisan W, Minoshima S. 3D-SSP analysis for amyloid brain PET imaging using [18F] florbetapir in patients with Alzheimer's dementia and mild cognitive impairment. Med J Malays. 2021;76(3):279–87.
45. Lundeen TF, Seibyl JP, Covington MF, Eshghi N, Kuo PH. Signs and artifacts in Amyloid PET. Radiographics. 2018;38:2123–33.
46. Nelissen N, Van Laere K, Thurfjell L, Owenius R, Vandenbulcke M, Koole M, et al. Phase 1 study of the Pittsburgh compound B derivative $^{18}$F-flutemetamol in healthy volunteers and patients with probable Alzheimer's disease. J Nucl Med. 2009;50:1251–9.